

## Design of mechanically-optimised lattice structures for vibration isolation

Wahyudin P. Syam<sup>1</sup>, Wu Jianwei<sup>2</sup>, Bo Zhao<sup>2</sup>, Ian Maskery<sup>3</sup>, Richard Leach<sup>1</sup>

<sup>1</sup>Manufacturing Metrology Team, Faculty of Engineering, The University of Nottingham, NG7 2RD, UK

<sup>2</sup>Ultra-Precision Optoelectronic Instrumentation Engineering Center, Harbin Institute of Technology, 150001, China

<sup>3</sup>Centre for Additive Manufacturing, Faculty of Engineering, The University of Nottingham, NG7 2RD, UK

[wahyudin.syam@nottingham.ac.uk](mailto:wahyudin.syam@nottingham.ac.uk)

**Abstract.** In this study, we investigate the use of additively manufactured strut-based lattice structures to enhance the mechanical vibration isolation properties of a structure. Three lattice designs, inspired by the common strut-based lattice structures, are presented. Design parameters to compare the lattice structures at the design stage are proposed. Finite element modelling has been used to determine the theoretical static and dynamic mechanical properties of both the single cell and the array configuration of the lattice structures. The lattices have been fabricated by selective laser sintering and experimentally tested to compare their static and dynamic properties to the theoretical model. A comparison and correlation of the static and dynamic properties of the lattice structures to the proposed design parameters are presented.

Additive manufacturing, lattice structures, metrology frame, vibration, natural frequency

### 1. Introduction

Additive manufacturing (AM) is, in general, limited by far fewer design constraints than conventional manufacturing processes, which gives AM the flexibility to produce freeform geometries [1]. The reduction of design constraints provides more options for designing mechanical parts used as structures, e.g. metrology frames and rotary equipment mounts (figure 1).

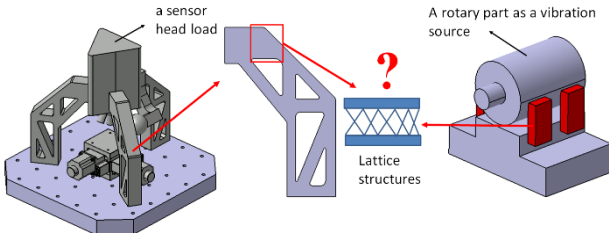


Figure 1. Illustrations of the use of lattice structures as structural supports for vibration isolation.

For many applications, it is desired that structures can be isolated from external vibration. Stiff structures are often used but essentially do not isolate vibration; rather they increase the natural frequency and affect the vibration damping. To have high-efficiency vibration isolation properties, a structure should have a low natural frequency ( $f_n$ ), which can be achieved by lowering its stiffness [2]. But, there is a practical limit: if the stiffness is too low, the structure will be unable to sustain the required mass load. Hence, there must be a trade-off between the stiffness and strength of the structure.

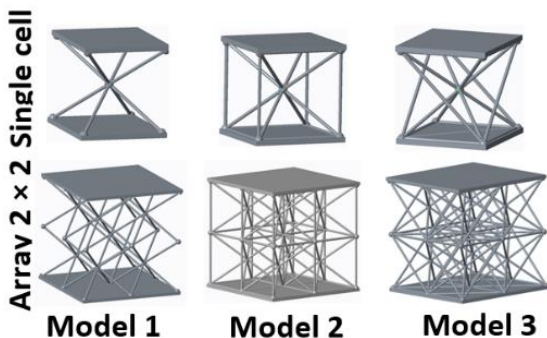


Figure 2. Three design of lattices. Row 1: in single cells. Row 2: in  $2 \times 2$  array configurations.

### 2. Lattice structure designs, analysis and simulation

Three designs of strut-based lattices are presented: model 1, model 2 and model 3, as shown in figure 2. Model 1 and model 2 are inspired by BCC and BCCz models (see [3] for details) and model 3 is a variation from model 1 and model 2. There are two types of design: a single cell (figure 3 top) and a  $2 \times 2$  array (figure 3 bottom).

Design parameters are used to compare the three lattice designs. The first parameters are the total moments of inertia  $I_x$  and  $I_y$  in the  $x$ - and  $y$ -axes, respectively, because  $f_n$  is directly proportional to  $I_x$  and  $I_y$  [2]. The other parameter is the Maxwell's criterion for strut-based structures [4]. The parameters consider that loads are applied vertically. The total moment of inertia is the sum over every strut in the lattice configuration.  $I_x$  and  $I_y$  for each strut are defined as:

$$I_{x,i} = [\cos \theta]^2 \frac{d_s l_s^3}{12} + [\sin \theta]^2 \frac{d_s^3 l_s}{12} + l_s d_s x_s^2, \quad (1)$$

$$I_{y,i} = [\cos \theta]^2 \frac{d_s^3 l_s}{12} + [\sin \theta]^2 \frac{d_s l_s^3}{12} + l_s d_s y_s^2 \quad (2)$$

where  $l_s$  is the length of the strut,  $d_s$  is the diameter of the strut  $i$ ,  $x_s$  and  $y_s$  are the distances of the centroid's axes of the strut  $i$  to the original  $O$   $x$ - and  $y$ -axes, respectively (figure 3) and  $\theta$  is the angle of the strut with respect to  $x$ -axis (figure 3).

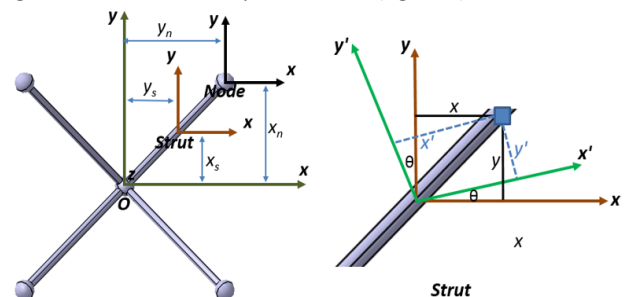


Figure 3. Variables used to calculate  $I_x$  and  $I_y$ .

The Maxwell's criterion is formulated as:

$$|N_{strut} - 3N_{node} + 6| \quad (3)$$

where  $N_{strut}$  and  $N_{node}$  are the number of struts and nodes, respectively. Equation (3) should be equated to zero so that a lattice structure is statically determined and to reduce the bending moment effect on each joint. The reduction of bending moments increases the compression strength of the lattice

structure. Table 1 shows the total moment of inertia and Maxwell's criterion for each of the lattice designs in the single cell configurations.

To estimate  $f_n$ , finite element analysis (FEA) was carried out by using ANSYS, and the FEA parameters are presented in table 1. The FEA results for  $f_n$  simulation are presented in figure 4. The single cell lattice is simulated in its original form to better compare with the calculated design parameters. As shown in figure 4, a thin plate is added to the design of the array configuration in order to place an accelerometer for vibration tests. For lattice vertical displacement predictions, a truss-matrix method is used considering a 5 N vertical force. From table 1, it can be seen that model 2 has the highest total moment of inertia and is expected to have the highest strength and  $f_n$ . Model 1 has the lowest total moment of inertia and the highest value of Maxwell's criterion, so it is expected to have the lowest strength and  $f_n$ . Finally, model 3 is expected to have strength and  $f_n$  that are in between model 1 and model 2 (table 1).

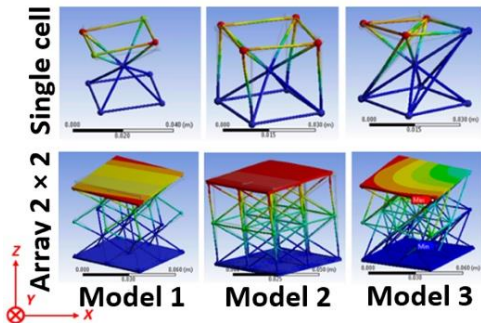


Figure 4. FEA simulation to estimate natural frequencies.

Table 1 Design parameters and simulation results.

Parameter	Single cell		
	Model 1	Model 2	Model 3
Total $I_x$ and $I_y / m^4$	0.2164	0.3444	0.3047
$ N_{strut} - 3N_{node} + 6 $	5	1	1
Natural frequency /Hz (FEM)	146.52	287.03	165.48
Maximum displacement in z-direction (FEM)	1.55	0.51	0.41

### 3. Experimental verification

The lattices were fabricated by selective laser sintering from Nylon-12 powder (figure 5). In order to measure  $f_n$ , additional thin plates are also added to the single cell lattice to place the sensor for impact tests. The impact test was carried out with two similar parts and three replications for each lattice type. Figure 6 shows the vibration signals of the lattices for model 1 (left), model 2 (centre) and model 3 (right). To measure the strength, compression tests were carried out with three replications for each lattice.

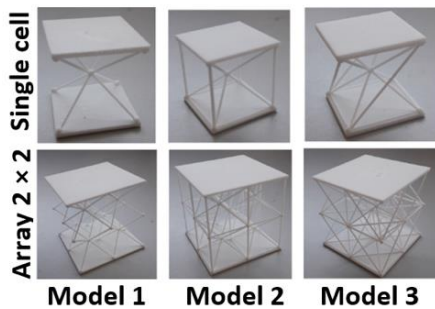


Figure 5. The fabricated lattices in single and array configuration.

The results of impact tests are presented in table 2. For single cells, minimum and maximum differences between experiment and simulation are 9.9 % and 17.2 %, respectively. For the array configuration, the minimum and maximum differences are 1.28 % and 14.2 %, respectively. The single cell results have larger differences since the simulation for the single cells are

without the thin plate structures. From the impact test, model 1 has the lowest  $f_n$ , while model 2 has the highest  $f_n$ .

Table 3 shows the results of the compression tests. Model 2 has the highest compression strength while model 1 has the lowest. From table 3, the maximum displacement at maximum force for model 1 (single cell) is 0.65 mm, while from the simulation the displacement is 1.55 mm. The higher displacement value of the simulation compared to the experiment suggests that model 1 cannot sustain the applied load because, at a displacement of 0.65 mm, the structure has undergone plastic deformation. Model 3 has a compression strength and  $f_n$  in between model 1 and model 2. Model 1 has the lowest  $f_n$  but cannot sustain the load. This suggests, for this type of load, model 3 can be selected as it has a sufficient strength but has a lower natural frequency compared to model 2, so that it has better vibration isolation properties, e.g. if the structure is used to sustain a linear motor that has typical frequency  $> 500$  Hz.

Table 2 Comparison of the natural frequencies of the lattice structures between FEM predictions and experiment results.

Type	Model	FEM /Hz	Experiment/Hz (mean value $\pm \sigma$ )	difference /%
Single Cell	Model 1	146.52	162.79 $\pm$ 8.67	9.99
	Model 2	287.03	308.09 $\pm$ 10.67	6.84
	Model 3	165.48	199.96 $\pm$ 9.61	17.24
2 x 2 Array	Model 1	47.55	49.77 $\pm$ 10.16	4.42
	Model 2	530.81	464.79 $\pm$ 47.41	14.20
	Model 3	324.79	320.70 $\pm$ 23.92	1.28

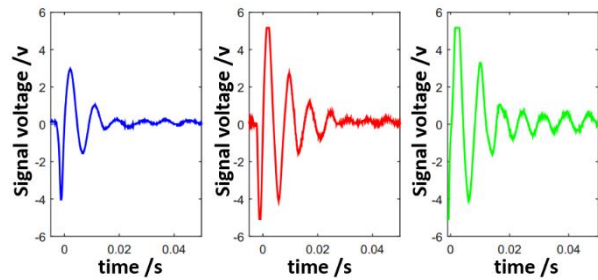


Figure 6. Signals from the impact tests for the single cells.

Table 3 Compression test results.

Model type	Max. force /N		Displacement at Max. force /mm	
	mean	$\pm \sigma$	mean	$\pm \sigma$
Model 1 single cell	2.45	0.23	0.65	0.16
Model 2 single cell	10.75	0.54	0.57	0.02
Model 3 single cell	4.32	0.30	0.42	0.01
Model 1 array 2 x 2	2.21	0.03	1.62	0.06
Model 2 array 2 x 2	19.25	0.08	0.68	0.08
Model 3 array 2 x 2	12.78	0.25	1.13	0.04

Comparing the simulation and experiment results, the proposed design parameters can be used as parameters for selecting a design of a strut-based lattice that has a vibration isolation property compromising between  $f_n$  and compression forces.

### 4. Conclusion and future challenges

The paper proposes design parameters that can be used to compare lattice designs, with regards to  $f_n$  and compression strength, to have vibration isolation properties. The parameters can be used as objectives for iterative optimisation processes to explore more feasible designs for vibration isolation.

Thanks to EPSRC (grant: EP/M008983/1) for funding this work.

### References

- [1] Thompson MK, et al. 2016 *Ann. CIRP* **65** 737-760
- [2] Schmitz T L, Smith K S 2012 *Mechanical vibrations: modelling and measurement* (Springer: New York)
- [3] Maskery I, et al. 2017 *J. Cell Plas.* in press.
- [4] Deshpande VS, et al. 2001 *Acta Mater.* **49** 1035-1040